

Explicit characterization of the identity configuration in an Abelian sandpile model

This article has been downloaded from IOPscience. Please scroll down to see the full text article.

2008 J. Phys. A: Math. Theor. 41 495003

(<http://iopscience.iop.org/1751-8121/41/49/495003>)

View [the table of contents for this issue](#), or go to the [journal homepage](#) for more

Download details:

IP Address: 171.66.16.152

The article was downloaded on 03/06/2010 at 07:22

Please note that [terms and conditions apply](#).

Explicit characterization of the identity configuration in an Abelian sandpile model

Sergio Caracciolo¹, Guglielmo Paoletti² and Andrea Sportiello¹

¹ Dip. Fisica, Università degli Studi di Milano and INFN, via G Celoria 16, 20133 Milano, Italy

² Dip. Fisica, Università di Pisa and INFN, largo B Pontecorvo 3, 56127 Pisa, Italy

Received 19 September 2008, in final form 5 October 2008

Published 29 October 2008

Online at stacks.iop.org/JPhysA/41/495003

Abstract

Since the work of Creutz, identifying the group identities for the Abelian sandpile model (ASM) on a given lattice is a puzzling issue: on rectangular portions of \mathbb{Z}^2 complex quasi-self-similar structures arise. We study the ASM on the square lattice, in different geometries, and a variant with directed edges. Cylinders, through their extra symmetry, allow an easy determination of the identity, which is a homogeneous function. The directed variant on square geometry shows a remarkable exact structure, asymptotically self-similar.

PACS numbers: 05.65.+b, 45.70.Qj, 64.60.Dc

Introduction

Bak, Tang and Wiesenfeld (BTW) introduced the Abelian sandpile model (with a different name) in [1] as a simple model for self-organized criticality. The model was soon generalized from the square lattice to arbitrary graphs [2]. It is a lattice automata, described in terms of local height variables $z_i \in \mathbb{N}$, i.e. the number of ‘particles’ at site i , so that a configuration is given by the set $C = \{z_i\}$. Particles fall into the system through a random memoryless process, and, as soon as some height z_i is higher than the local threshold value \bar{z}_i , it *topples* to the neighbouring sites, i.e. the value z_i decreases by the (integer) amount Δ_{ii} , while, for each site $j \neq i$, increases by the (integer) amount $-\Delta_{ij}$. This relaxation process (the *avalanche*) is guaranteed to stop in a finite number of steps if $b_i^- := \sum_j \Delta_{ij} \geq 0$ for all sites i , and a certain technical condition is satisfied (the matrix Δ must be a *strictly dissipative* diffusion kernel). All the heights remain non-negative if this is the case in the starting configuration, and $\bar{z}_i \geq \Delta_{ii}$. For future convenience we also define $b_i^+ := \sum_j \Delta_{ij}^T$, and assume also that these quantities be non-negative.

A graph, in general directed and with multiple edges, is thus defined through the non-diagonal part of $-\Delta$, seen as an adjacency matrix, while the non-zero values b_i^\pm are regarded as (in- or out-coming) ‘connections to the border’ (and the sites i with b_i^+ or b_i^- non-zero are

said to be ‘on the border’). If Δ is symmetric, we have an undirected graph, and automatically $b_i^+ = b_i^-$. We just write b_i for b_i^+ and b_i^- when clear that they are equal.

This is the case in the original BTW model, which is defined on a portion of the \mathbb{Z}^2 lattice. We have in this case $\bar{z}_i = \Delta_{ii} = 4$ on each site, and $\Delta_{ij} = -1$ on all pairs of neighbouring sites. If we are on a rectangular domain, say of sides L_x and L_y , we have $b_i = 1$ for vertices on the sides of the rectangle, and $b_i = 2$ for the corners.

In [1] it is described how, already for this case, the avalanches show an unpredictable dynamics, with power-law size distribution, which candidated the model as a toy description of many interesting features, such as the $1/f$ noise.

Afterwards, Dhar and collaborators, in a series of relevant works [2–4], elucidated a deep structure of the Markov chain related to the general ASM: the set of *stable* configurations $S = \bigotimes_i \{0, 1, \dots, \bar{z}_i - 1\}$, those where no toppling can occur, is divided into a set T of *transient* and a set R of *recurrent* ones, the latter being visited an infinite number of times by the chain, and forming a single ergodic basin. Given the natural partial ordering, $C \preceq C'$ iff $z_i \leq z'_i$ for all i , then R is in a sense ‘higher’ than T , more precisely

$$\nexists (C, C') \in T \times R : \quad C > C'; \tag{1}$$

$$\forall C \in T \quad \exists C' \in R : \quad C < C'. \tag{2}$$

In particular, the *maximally-filled* configuration $C_{\max} = \{\bar{z}_i - 1\}$ is in R , and higher than any other stable configuration.

The set R has an underlying Abelian structure, for which a presentation is explicitly constructed in terms of the matrix Δ , through the (heavy) study of its Smith normal form. Shortcuts of the construction and more explicit analytical results are achieved in the special case of a rectangular $L_x \times L_y$ portion of the square lattice, and still stronger results are obtained for the case of $L_x = L_y$ [4].

Call \tilde{a}_i the operator which adds a particle at site i to a configuration C , and a_i the formal operator which applies \tilde{a}_i , followed by a sequence of topplings which makes the configuration stable. Remarkably, the final configuration $a_i C$ is independent from the sequence of topplings, and also, applying two operators, the two configurations $a_j a_i C$ and $a_i a_j C$ coincide, so that at a formal level a_i and a_j do commute.

More precisely, if a_i acting on C consists of the fall of a particle in i , \tilde{a}_i , and the sequence of topplings t_{i_1}, \dots, t_{i_k} on sites i_1, \dots, i_k , the univocal definition of a_i and the commutation of a_i and a_j follow from the two facts:

$$z_j \geq \bar{z}_j : \quad t_j \tilde{a}_i C = \tilde{a}_i t_j C; \tag{3}$$

$$z_i \geq \bar{z}_i \text{ and } z_j \geq \bar{z}_j : \quad t_i t_j C = t_j t_i C. \tag{4}$$

Another consequence is that, instead of doing all the topplings immediately, we can postpone some of them after the following \tilde{a} ’s, and still get the same result. Similar manipulations show that the relation

$$a_i^{\Delta_{ii}} = \prod_{j \neq i} a_j^{-\Delta_{ij}} \tag{5}$$

holds when applied to an arbitrary configuration.

These facts lead to the definition of an Abelian semi-group operation between two configurations, as the sum of the local height variables z_i , followed by a relaxation process [5]:

$$C \oplus C' = \left(\prod_i a_i^{z_i} \right) C' = \left(\prod_i a_i^{z'_i} \right) C. \tag{6}$$

For a configuration C , we define multiplication by a positive integer:

$$kC = \underbrace{C \oplus \cdots \oplus C}_k. \tag{7}$$

The set R of recurrent configurations is special, as each operator a_i has an inverse in this set, so the operation above, restricted to R , is raised to a group operation. According to the fundamental theorem of finite Abelian groups, any such group must be a ‘discrete torus’ $\mathbb{Z}_{d_1} \times \mathbb{Z}_{d_2} \times \cdots \times \mathbb{Z}_{d_g}$, for some integers $d_1 \geq d_2 \geq \cdots \geq d_g$, and such that $d_{\alpha+1}$ divides d_α for each $\alpha = 1, \dots, g-1$. The values d_α , called *elementary divisors* of Δ , and a set of generators e_α with the proper periodicities, can be constructed through the normal form decomposition [4]. The composition of whatever $C = \{z_i\}$ with the set R acts then as a translation on this toroidal geometry. A further consequence is that, for any recurrent configuration C , the inverse configuration $(-C)$ is defined, so that kC is defined for $k \in \mathbb{Z}$.

Consider the product over sites i of equation (5)

$$\prod_i a_i^{\Delta_{ii}} = \prod_i \prod_{j \neq i} a_j^{-\Delta_{ij}} = \prod_i a_i^{-\sum_{j \neq i} \Delta_{ji}}. \tag{8}$$

On the set R , the inverses of the formal operators a_i are defined, so that we can simplify common factors in (8), recognize the expression for b^+ , and get

$$\prod_i a_i^{b_i^+} = I \tag{9}$$

so that $\prod_i a_i^{b_i^+} C = C$ is a necessary condition for C to be recurrent (but it is also sufficient, as no transient configuration is found twice in the same realization of the Markov chain), and goes under the name of *identity test*.

This condition turns into an equivalent and computationally cheaper procedure, called *burning test*, of which a side product, in the case of a positive answer, is a spanning arborescence rooted on the vertices of the border. So, the burning test provides us a bijection between the two ensembles, of recurrent sandpile configurations and rooted arborescences with roots on the border. This is in agreement with the Kirchhoff matrix-tree theorem, which states that the number of such arborescences is given by $\det \Delta$, while the number of recurrent configurations is known to be $\det \Delta$ as the first step of the procedure which determines the elementary divisors d_α [3].

If, for the graph identified by Δ , a planar embedding exists, with all sites i such that $b_i^+ > 0$ on the most external face, then the planar dual of a rooted arborescence coming from the burning test is a spanning tree on the planar-dual graph.

This is clear for the undirected case $\Delta = \Delta^T$, and needs no more words. If the graph is directed, the arborescence is directed in the natural way, while the dual tree is constrained in some complicated way (some combinations of edge-occupations are forced to fixed values). However, the graphical picture simplifies if, on the planar embedding, in-coming and out-coming edges are cyclically alternating (and all plaquettes have consistent clockwise or counter-clockwise perimeters), and all sites with either b^+ or b^- positive are on the most external face, with in- and out-going arrows cyclically alternating (cf, for example, figure 1).

We will call a directed graph of this kind a *planar alternating directed graph*.

The connection with uniform spanning trees and the Kirchhoff theorem explains *a posteriori* the arising of self-organized criticality, i.e. the appearance of long-range behaviour with no need of tuning any parameter. Indeed, uniform spanning trees on regular two-dimensional lattices are a $c = -2$ logarithmic conformal field theory (CFT), and have no parameter at all, being a peculiar limit $q \rightarrow 0$ of the Potts model in the Fortuin–Kasteleyn

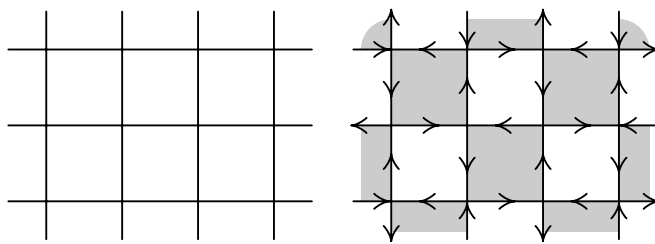


Figure 1. Left: a portion of the square lattice. Right: a portion of the directed square lattice we considered in this work, with in- and out-edges alternated cyclically, and white and grey faces with arrows oriented clockwise and counter-clockwise.

formulation [6], or a limit of zero curvature in the $OSP(1|2)$ nonlinear σ -model [7]. If instead one considers the larger ensemble of spanning forests, in a parameter t counting the components (or describing the curvature of the $OSP(1|2)$ supersphere), the theory in two dimensions is scale-invariant for three values: at $t = 0$ (the spanning trees, or the endpoint of the ferromagnetic critical line of Potts), at the infinite-temperature point $t = \infty$, and at some non-universal negative t corresponding to the endpoint of the anti-ferromagnetic critical line of Potts, being $t_c = -1/4$ on the square lattice. Through the correspondence with the nonlinear σ -model, one can deduce at a perturbative level the renormalization group flow, and, in particular, that the system is asymptotically free for $t > 0$ [7, 8], so that $t = 0^+$ is an ultraviolet fixed point.

An interesting connection between the height variables in the ASM and the fields of the underlying CFT is performed in [3, 9–11], and especially in [11].

Identities

Given the algebraic relation (9), and the semi-group operation (6), one could define the *frame* configuration Id_f as that with $z_i = b_i^+$ for all i , and realize that it acts as an identity on recurrent configurations, $Id_f \oplus C = C$ if $C \in R$. Conversely, in general it does not leave unchanged a transient configuration, and in particular, as, for any relevant extensive graph, Id_f is itself transient, we have that $Id_f \oplus Id_f$, and $Id_f \oplus Id_f \oplus Id_f$, and so on, are all different, up to some number of repetitions k at which the configuration is sufficiently filled up with particles to be recurrent. We call Id_r this configuration, and $k(\Delta)$ the minimum number of repetitions of Id_f required in the ASM identified by Δ (we name it the *filling number* of Δ). The configuration Id_r is the identity in the Abelian group $\mathbb{Z}_{d_1} \times \dots \times \mathbb{Z}_{d_g}$ described above, and together with a set of generators e_α , completely identifies in a constructive way the group structure of the statistical ensemble. The relevance of this configuration has been stressed first by Creutz [5], so that we shall call it *Creutz identity*. See figure 2 for an example.

Unfortunately, despite many efforts, it has not been possible to give a closed-formula recipe for this identity state on given large lattices, not even in the case of a $L \times L$ square, and the direct numerical investigation of these configurations at various sizes has produced peculiar puzzling pictures [12].

In a large-side limit, we have the formation of curvilinear triangular regions of extensive size (of order L), filled with regular patterns, and occasionally crossed by straight ‘defect lines’, of widths of order 1, which, furthermore, occasionally meet at Y-shaped ‘scattering points’, satisfying peculiar conservation laws [13].

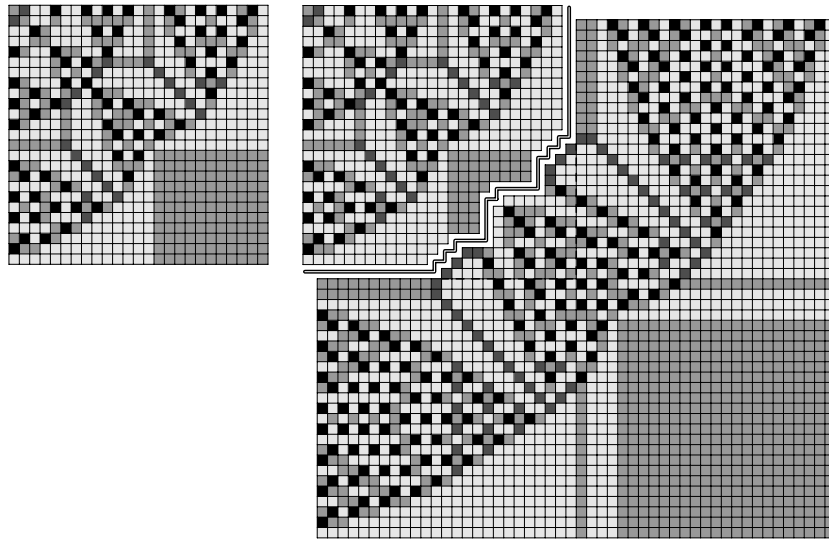


Figure 2. The top-left corners of the identities $Id_r^{(L)}$ for $L = 50$ and $L = 100$ in the BTW model (the other quadrants are related by symmetry). Heights from 0 to 3 correspond to grey tones from dark to light. The smaller-size identity is partially reproduced at the corner of the larger one, in a fashion which resembles the results of theorem 1.

Table 1. Values of k_L for the BTK Abelian sandpile on square geometries of even size, for $L = 2, \dots, 64$.

L	2	4	6	8	10	12	14	16	18	20	22	▷
k_L	1	4	7	13	19	27	35	46	58	71	87	▶
▷	24	26	28	30	32	34	36	38	40	42	44	▷
▶	103	119	138	156	180	198	226	248	276	305	334	▶
▷	46	48	50	52	54	56	58	60	62	64		
▶	367	397	430	464	499	538	572	615	653	699		

Similar features emerge also for the filling numbers, e.g. on the square lattice of size L , the index $k_L \equiv k(\Delta^{(L)})$ is not badly fitted, for even L , by a parabola $k_L \simeq L^2/6 + o(L^2)$, but showing fluctuations due to unpredictable number-theoretical properties of L . The challenging sequence of these numbers, for L up to 64, is given in table 1. It should be noted that, conversely, odd sizes $2L + 1$ are related to $2L$ through a property proven in [4, section 7].

The determination of Id_r for a given graph is a procedure polynomial in the size of the graph. For example, one could prove that $k(\Delta)$ is sub-exponential, and that relaxing $C \oplus C'$ for C and C' both stable is polynomial, then one can produce the powers $2^s Id_r$ recursively in s , to get twice the same configuration. Better algorithms exist however, see for example [5].

Still, one would like to have a better understanding of these identity configurations. This motivates us to the study of the ASM on different regular graphs, such that they resemble, as much as possible, the original model, but simplify the problem in some regards so that the family (over L) of resulting identities can be understood theoretically.

In this research, we keep in mind a few principles: (1) we wish to simplify the problem in some structural way; (2) we want to preserve the property of the $L \times L$ lattice, discussed in

[4, section 4], of reconstruction of the elementary divisors of Δ from a suitable matrix $n_{yy'}$, outcome of a machinery for producing an ‘economic’ presentation of the group, in terms of $\mathcal{O}(L)$ generators a_i of the whole set of L^2 ; (3) possibly, we want to preserve planarity, and the interpretation of dual spanning subgraphs as spanning trees on the dual lattice, i.e. we want to use either planar undirected graphs, or planar alternating directed graphs (according to our definition above).

A prolog: cylindric geometries

A first possible simplification comes from working on a cylindrical geometry. We call respectively *periodic*, *open* and *closed* the three natural conditions on the boundaries of a $L_x \times L_y$ rectangle. For example, in the BTW Model, for site $(i, 1)$, in the three cases of periodic, open and closed boundary conditions on the bottom horizontal side we would have the following toppling rules:

$$\begin{array}{lll}
 \text{periodic:} & z_{i,1} \rightarrow z_{i,1} - 4; & z_{i\pm 1,1} \rightarrow z_{i\pm 1,1} + 1; \\
 & z_{i,2} \rightarrow z_{i,2} + 1; & z_{i,L_y} \rightarrow z_{i,L_y} + 1; \\
 \text{open:} & z_{i,1} \rightarrow z_{i,1} - 4; & z_{i\pm 1,1} \rightarrow z_{i\pm 1,1} + 1; \\
 & z_{i,2} \rightarrow z_{i,2} + 1; & \\
 \text{closed:} & z_{i,1} \rightarrow z_{i,1} - 3; & z_{i\pm 1,1} \rightarrow z_{i\pm 1,1} + 1; \\
 & z_{i,2} \rightarrow z_{i,2} + 1. &
 \end{array}$$

The external face, with $b_i^\pm \neq 0$, is in correspondence of open boundaries, so, as we want a single external face, if we take periodic boundary conditions in one direction (say, along x), the only possible choice in this framework is to take closed and open conditions on the two sides in the y direction.

Our notation is that \bar{z}_i takes the same value everywhere: on open boundaries, b_i^- and b_i^+ are determined accordingly, while on closed boundaries either we add some extra ‘loop’ edges, or we take $\bar{z}_i - \Delta_{ii} > 0$.

The cylindric geometry has all the non-trivial features of the original ASM for what concerns group structures, polynomial bound on the relaxation time in the group action, connection with spanning trees, and so on (even the finite-size corrections to the continuum-limit CFT are not more severe on a $L_x \times L_y$ cylinder than on a $L_x \times L_y$ open-boundary rectangle), *but*, for what concerns the determination of Id_r through relaxation of kId_i , the system behaves as a quasi-unidimensional one, and Id_r is in general trivially determined.

Furthermore, in many cases Id_r is just the maximally-filled configuration C_{\max} . This fact is easily proven, either by checking that $Id_r \oplus Id_i = Id_r$, which is easy in the quasi-one-dimensional formulation (or in other words, by exploiting the translation symmetry in one direction), or with a simple burning-test argument, in the cases in which on each site there is a single incoming edge from sites nearer to the border. Figure 3 shows a few examples.

Such a peculiar property has a desirable consequence on the issue of inversion of a recurrent configuration. Indeed, if C and C' are in R , we have that

$$(-C) \oplus C' = Id_r \oplus (-C) \oplus C' = (Id_r - C) \oplus C' \tag{10}$$

where, if $C = \{z_i\}$, $(-C) = \{\tilde{z}_i\}$ is the inverse configuration we seek, but $Id_r - C$ is simply the configuration with $\tilde{z}_i = \bar{z}_i - z_i - 1$, and has all non-negative heights.

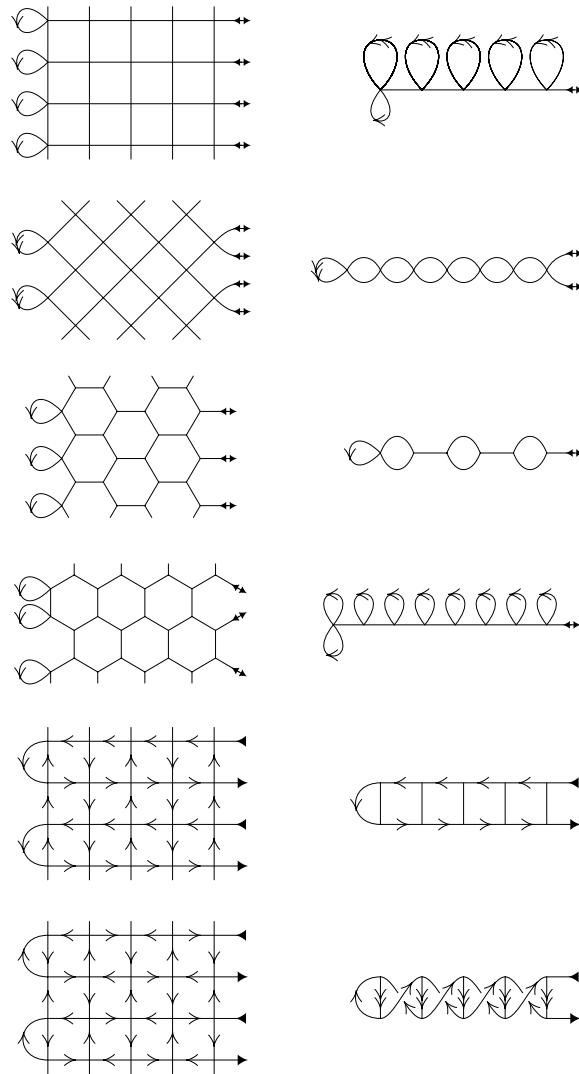


Figure 3. Reduction to a quasi-one-dimensional system for the ASM on cylindrical geometry, on a few examples all having Id_r coinciding with C_{\max} . From top to bottom: a portion of the square lattice, in the two orientations; of the hexagonal lattice, in the two orientations, of Manhattan and pseudo-Manhattan lattices. Plain edges correspond to $\Delta_{ij} = \Delta_{ji} = -1$, while a directed edge (from i to j) with k arrows corresponds to $\Delta_{ij} = -k$. In-(out-)coming bold arrows correspond to b^- (b^+) equal to 1, while the lozenge-shaped double-arrows correspond to $b^- = b^+ = 1$. A loop with k arrows on i corresponds to $\bar{z}_i - \Delta_{ii} = k$, otherwise $\bar{z}_i = \Delta_{ii}$.

Pseudo-Manhattan lattice

From this section on, we will concentrate on square geometries, on the square lattice with edges having a given orientation, and all vertices having in- and out-degree equal to 2.

For this reason, we can work with $\bar{z}_i = 2$, so that $S = \{0, 1\}^V$ instead of $\{0, 1, 2, 3\}^V$ (a kind of simplification, as from ‘CMYK’ colour printing to ‘black and white’). In this step we

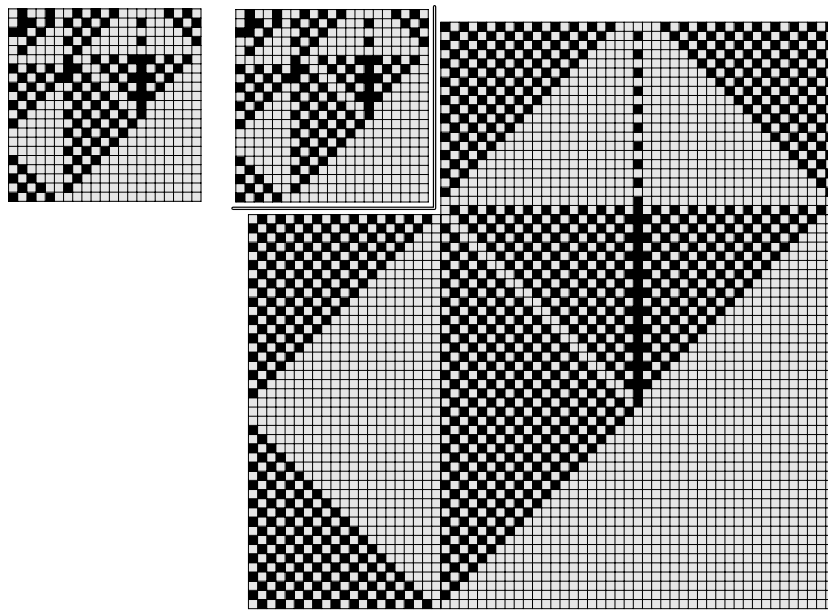


Figure 4. The top-right corners of the identities $Id_r^{(L)}$ for $L = 21$ and $L = 64$ (remark: $64 = 3 \times 21 + 1$). The smaller-size one is exactly reproduced at the corner of the larger one, while the rest of the latter has an evident regular structure, according to theorem 1.

lose in general a bit of symmetry: e.g. on a square of size $2L$ we have still the four rotations, but we lose the reflections, which are arrow-reversing, while on a square of size $2L + 1$ we lose rotations of an angle $\pi/2$, and only have rotation of π .

Square lattices with oriented edges have already been considered in statistical mechanics, especially in the variant called the ‘Manhattan lattice’ (i.e. with horizontal edges oriented east- and west-bound alternately on consecutive rows, and coherently within a row, and similarly for vertical edges), cf, for example, [14]. However this lattice in two dimensions is not a planar alternating directed graph, and the results for the related ASM model will be discussed only briefly in the last section.

We start by analysing a less common variant, which is better behaving for what concerns the ASM model, and which we call *pseudo-Manhattan lattice* (it appears, for example, in the totally unrelated paper [15]). In this case, the horizontal edges are oriented east- and west-bound alternately in both directions (i.e. in a chequer design), and similarly for vertical edges. As a result, all plaquettes have cyclically oriented edges. A small portion of this lattice is shown in figure 1, where it is depicted indeed as the prototype planar alternating directed graph. Conventionally, in all our examples (unless otherwise specified) we fix the orientations at the top-right corner to be as in the top-right corner of figure 1.

Quite recently, in [19] both Manhattan and pseudo-Manhattan lattices have been considered as an interesting variant of the ASM model (the latter under the name of *F-lattice*), with motivations analogous to ours. This corroborates our claim that these variants are natural simplifications of certain features in the original BTK model.

The main feature of the Creutz identities, on square portions of the pseudo-Manhattan lattice with even side, is self-similarity for sides best approximating the ratio $1/3$, up to a trivial part, as illustrated in figure 4.

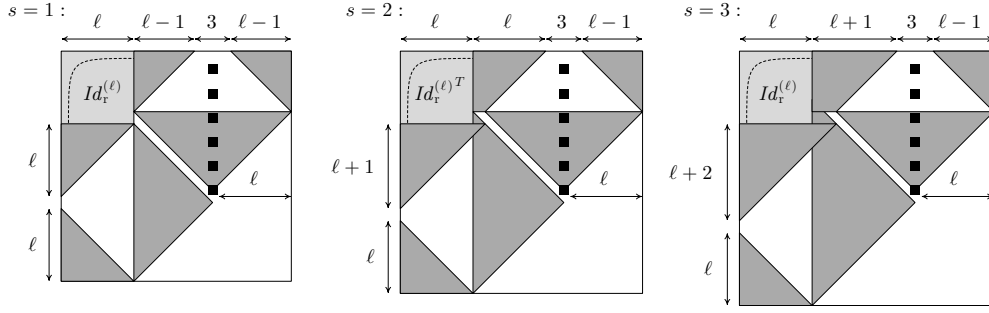


Figure 5. The non-recursive part of the identities $Id_r^{(L)}$ (top-right corners) for $L = 3\ell + s$, and $s \in \{1, 2, 3\}$, illustrating the set described by (11). For $s = 2$, we show the transposed of Id_r . Black and white stand respectively for $z_i = 0$ and 1; grey regions correspond to chequered parts, starting with white on the cells cutted by $\pi/4$ -inclination lines.

The precise statement is in the following theorem 1. Call $Id_r^{(L)}$ the set of heights in the Creutz identity for the square of side $2L$, encoded as a $L \times L$ matrix for one of the four portions related by rotation symmetry. Say that index $(1, 1)$ is at a corner of the lattice, and index (L, L) is in the middle. We have

Theorem 1. Say $L = 3\ell + s$, with $s = 1, 2, 3$. Then, $Id_r^{(L)}$ is determined from $Id_r^{(\ell)}$ and a closed formula, and thus, recursively, by a deterministic telescopic procedure in at most $\lceil \log_3 L \rceil$ steps.

For $s = 1$ or 3 , we have $(Id_r^{(L)})_{ij} = (Id_r^{(\ell)})_{ij}$ if $i, j \leq \ell$, otherwise $(Id_r^{(L)})_{ij} = 0$ iff, for $i + j + s$ even,

$$i < \ell, \quad |L - \ell - j| - i > 0; \tag{11a}$$

$$j > \ell, \quad |2\ell + 1 - i| + j < 2\ell + s; \tag{11b}$$

$$i \leq 2\ell, \quad j = L - \ell; \tag{11c}$$

and, for $i + j + s$ odd,

$$i > \ell, \quad |L - \ell - i| - j > 0; \tag{11d}$$

$$i > \ell - 1, \quad |2\ell + s - j| + i < 2\ell. \tag{11e}$$

If $s = 2$ the same holds with i and j transposed in $Id_r^{(L)}$ and $Id_r^{(\ell)}$ (but not in (11)). Furthermore, $k_L = \frac{L(L+1)}{2}$.

The statement of equations (11) is graphically represented in figure 5.

The understanding of the Creutz identity on square portions of the pseudo-Manhattan lattice is completed by the following theorem, relating the identity at side $2L + 1$ to that at side $2L$. We encoded the identity at even sides in a $L \times L$ matrix $Id_r^{(L)}$, exploiting the rotation symmetry, such that the extended $2L \times 2L$ matrix has the property

$$(Id_r^{(L)})_{i,j} = (Id_r^{(L)})_{2L+1-j,i}. \tag{12}$$

We can similarly encode the identity at odd sides in a structure of almost 1/4 of the volume, namely a $(L + 1) \times (L + 1)$ matrix $\hat{Id}_r^{(L)}$, using the fact that

$$(\hat{Id}_r^{(L)})_{i,j} = (\hat{Id}_r^{(L)})_{2L+2-i,j} = (\hat{Id}_r^{(L)})_{i,2L+2-j}. \tag{13}$$

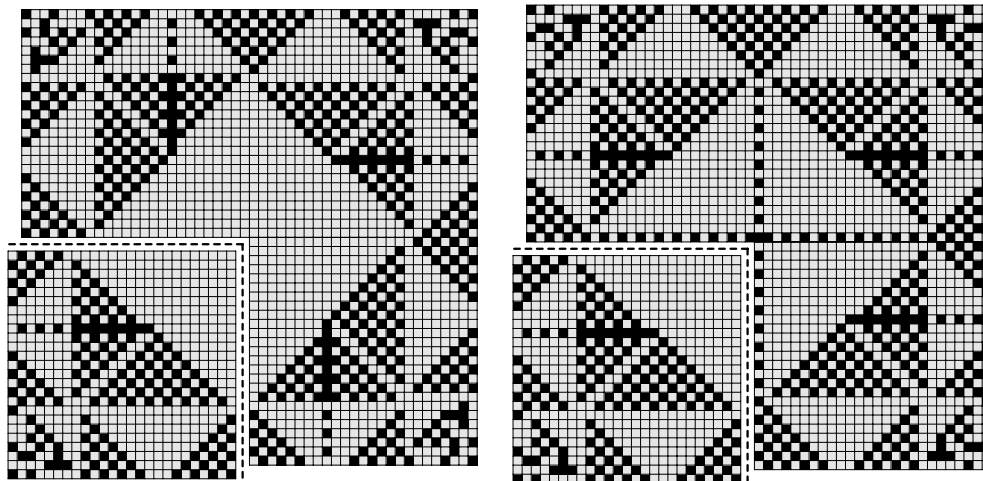


Figure 6. The recurrent identity on the pseudo-Manhattan lattice of side 50 (up) and 51 (down), an example of how the identity on side $2L + 1$ is trivially deduced from that on side $2L$.

Theorem 2. We have $(\hat{Id}_r^{(L)})_{i,j} = (Id_r^{(L)})_{i,j}$ if $i, j \leq L$, $(\hat{Id}_r^{(L)})_{L+1,j} = 0$ if $L - j$ is odd and 1 if it is even, and, for $i \leq L$, $(\hat{Id}_r^{(L)})_{i,L+1} = 0$ if $L - i$ is even and 1 if it is odd.

The statement of this theorem is illustrated in figure 6.

The proof of theorem 2, given theorem 1, is easily achieved through arguments completely analogous to those of [4, section 7]. We postpone the (harder) proof of theorem 1 to the discussion of the equivalence with theorem 4 below.

There are some similarities and differences with the identities in the BTW model. In that case, besides the evident height-2 square in the middle, there arise some curvilinear triangular structures, mostly homogeneous at height 3, but some others ‘texturized’, so that there exists a variety of patterns which appear extensively at large sizes (in the metaphor of CMYK offset printing, like the way in which composite colours are produced!). A first attempt of classification of these structures appears in [18]. In our case, we only have ‘black and white’, but, as four zeroes in a square are a forbidden configuration (as well as many others too dense with zeroes), we cannot have extensive regions of zeroes (black, in our drawings of figure 4). A big square in the middle is still there, rotated by 45 degrees, while triangoloids are replaced by exact ‘45–45–90’ right triangles in a ‘texturized grey’ coming from a chequered pattern. Indeed, to our knowledge, such a regular structure as in theorem 1 was not deducible *a priori* (in particular, not before the publication of [19]), and our initial motivation was to study the emergence of patterns in a 2-colour case.

The statement of theorem 1 would suggest to look for similar features also in the BTW model. It turns out that, while in the directed case the $\lfloor(L - 1)/3\rfloor$ size is *fully* contained in the corner of the L size, in the BTW the $\lfloor L/2\rfloor$ size is *partially* contained in the corner of the L size, in an empirical way which strongly fluctuates with L , but is in most cases more than 50% (cf figure 2 for an example).

The heuristics in the case of the Manhattan lattice, under various boundary prescriptions, are somewhat intermediate: the continuum-limit configuration exists and coincides with that

for the pseudo-Manhattan, but the $\lfloor(L - 1)/3\rfloor$ corners are only partially reproduced by the size- ℓ identities.

How could one prove theorem 1? An elegant algebraic property of the identity is that it is the only recurrent configuration for which all the ‘charges’ are zero (see [4], equations (3.3) and (3.4)). More precisely, and in a slightly different notation, given a whatever ordering of the sites, and any site i , and calling $A_{i,j}$ the minor (i, j) of a matrix A , we have

$$Q_j(C) := \sum_i z_i (-1)^{i+j} \det \Delta_{i,j} \tag{14}$$

and $Q_j(Id_r) = q_j \det \Delta$ with $q_j \in \mathbb{Z}$, with Id_r being the only stable recurrent configuration with this property.

A possible proof direction (that we do *not* follow in this paper) could have been as follows. An algebraic restatement of the expression for the charges is achieved in Grassmann calculus, through the introduction of a pair of anticommuting variables $\bar{\psi}_i, \psi_i$ per site. Then, by Grassmann Gaussian integration, we have that

$$(-1)^{i+j} \det \Delta_{i,j} = \int \mathcal{D}(\psi, \bar{\psi}) \bar{\psi}_i \psi_j e^{\bar{\psi} \Delta \psi} \tag{15}$$

where there is a contribution $b_k^- \bar{\psi}_k \psi_k$ in the exponential for each site on the border, and a contribution $(\bar{\psi}_h - \bar{\psi}_k) \psi_k$ if a particle falls into h after a toppling in k , i.e. $\Delta_{hk} = -1$ (we are pedantic on this because the asymmetry of Δ could create confusion on who’s who with $\bar{\psi}$ and ψ).

So the configurations in the same equivalence class of the identity are the only ones such that, for each j , the ‘expectation value’

$$\left\langle \left(\sum_i z_i \bar{\psi}_i \right) \psi_j \right\rangle := \frac{\int \mathcal{D}(\psi, \bar{\psi}) \left(\sum_i z_i \bar{\psi}_i \right) \psi_j e^{\bar{\psi} \Delta \psi}}{\int \mathcal{D}(\psi, \bar{\psi}) e^{\bar{\psi} \Delta \psi}} \tag{16}$$

is integer-valued.

Furthermore, expressions as on the right-hand side of (15) are related, through the Kirchhoff theorem, to the combinatorics of a collection of directed spanning trees, all rooted on the boundary, with the exception of a single tree which instead contains both i and j , and the path on the tree from i to j is directed consistently.

So, a possible approach by combinatorial bijections could be to prove that, for any j , there is a suitable correspondence among the forests as above, and a number q_j of copies of the original ensemble of rooted forests.

Such a task is easily performed, even for a generic (oriented) graph, for what concerns the frame identity Id_f , for which all charges q_j are 1. Unfortunately, for what concerns Id_r , and with an eye to the proof performed in the following section, it seems difficult to pursue this project at least in the case of the pseudo-Manhattan lattice on a square geometry. Indeed, if the relaxation of $k_L Id_f$ to Id_r requires t_j topplings on site j , it is easy to see that $q_j(Id_r) = k_L - t_j$, and from the explicit expressions for k_L and the values of the topplings (the latter are in the following theorem 4) we see that the values of the charges q_j are integers of order L^2 .

Proof of the theorem

Here we perform the direct proof of theorem 1. It is fully constructive, a bit technical, and maybe not specially illuminating for what concerns the algebraic aspects of the problem, but still, it does the job.

Now, in order to better exploit the geometry of our square lattice, we label a site through a pair ij denoting its coordinates. We can introduce the matrix $T_{ij}^{(L)}$, which tells how many

topplings site ij performed in the relaxation of $k_L Id_f$ into Id_r . Exploiting the rotational symmetry, we take it simply $L \times L$ instead of $2L \times 2L$, with $(i, j) = (1, 1)$ for the site at the corner, analogously to what we have done for $(Id_r^{(L)})_{ij}$. Of course, although we call $T^{(L)}$ and $Id_r^{(L)}$ ‘matrices’, they have a single site-index, and are indeed vectors, for example, under the action of Δ .

Clearly, T is a restatement of Id_r as

$$(Id_r^{(L)})_{ij} = k_L b_{ij}^+ - \Delta_{ij,i'j'} T_{i'j'}^{(L)} \tag{17}$$

so that Id_r is determined from T , but also vice-versa, as Δ is invertible. Actually, through the locality of Δ , one can avoid matrix inversion if one has some ‘boundary condition’ information on T , and the exact expression for Id_r , e.g. if one knows T on two consecutive rows and two consecutive columns (and we have a guess of this kind, as we discuss in the following).

The constraint that $(Id_r)_{ij} \in \{0, 1\}$ gives that T is locally a parabola with small curvature. Moreover, in the regions corresponding to homogeneous portions of Id_r , T must correspond to a discretized parabola through easy formulae. The telescopic nature of $(Id_r^{(L)}, Id_r^{(\lfloor \frac{L-1}{3} \rfloor)}, \dots)$ has its origin in an analogous statement for $(T^{(L)}, T^{(\lfloor \frac{L-1}{3} \rfloor)}, \dots)$, and on the fact that k_L has a simple formula. As we will see, these facts are easier to prove.

We start by defining a variation of T which takes into account explicitly both the height-1 square in the middle of Id_r , and the spurious effects on the border. Define $\tilde{k}(L) = \lfloor (L-1)(L+2)/4 \rfloor$ (which is approximatively $k_L/2$), and introduce

$$\hat{T}_{ij}^{(L)} := T_{ij}^{(L)} - \tilde{k}(L) b_{ij}^+ - \binom{L-i+1}{2} - \binom{L-j+1}{2}. \tag{18}$$

A first theorem is that

Theorem 3.

$$\hat{T}_{iL}^{(L)} = \hat{T}_{Lj}^{(L)} = 0; \tag{19a}$$

$$\hat{T}_{ij}^{(L)} = 0 \quad \text{for } i+j > L+\ell; \tag{19b}$$

$$\hat{T}_{ij}^{(L)} \leq 0 \quad \text{for all } i, j. \tag{19c}$$

This implicitly restates the claim about the middle square of height 1 in Id_r , and is in accord with the upper bound on the curvature of T given by $(Id_r)_{ij} \leq 1$. With abuse of notations, we denote by $\hat{T}_{ij}^{(\ell)}$ also the $L \times L$ matrix corresponding to $\hat{T}_{ij}^{(\ell)}$ in the $\ell \times \ell$ corner with $i, j \leq \ell$, and zero elsewhere. Then the rephrasing of the full theorem 1 gives

Theorem 4. *If $M_{ij}^{(L)} = -(\hat{T}_{L-iL-j}^{(L)} - \hat{T}_{L-iL-j}^{(\ell)})$ for $s = 1, 3$ and the transpose of the latter for $s = 2$, defining $\theta(n) = 1$ for $n > 0$ and 0 otherwise, and the ‘quadratic + parity’ function $q(n)$ on positive integers*

$$q(n) = \theta(n) \left(n^2 + 2n + \frac{1 - (-1)^n}{2} \right) = \begin{cases} 0 & n \leq 0; \\ (n+1)^2/4 & n \text{ positive odd}; \\ n(n+2)/4 & n \text{ positive even}; \end{cases} \tag{20}$$

then $M^{(L)}$ is a deterministic function, piecewise ‘quadratic + parity’ on a finite number of triangular patches

$$\begin{aligned}
 M_{ij}^{(L)} = & \theta(i-L+\ell) \left[-\binom{j}{2} - \max(0, j-\ell-1) + q(j-i+L-\ell) - q(j+i-L-\ell-4) \right] \\
 & + \theta(j-L+\ell) \left[-\binom{i}{2} - \theta(L-\ell-i+1) + q(i-j+L-\ell-1) \right. \\
 & \left. + q(i+j-L+\ell-2) + q(i+j-L-\ell-3) \right]. \tag{21}
 \end{aligned}$$

Clearly theorem 3 is contained in theorem 4, just by direct inspection of the summands in (21). The equivalence among theorems 1 and 4 is achieved still by direct inspection of (21), with the help of some simple lemmas. First remark that the use of $-\hat{T}$ instead of T makes us work ‘in false colours’, i.e. effectively interchanges z into $1-z$ in Id_r . Then, defining $\nabla_x^2 f(i, j) := f(i+1, j) + f(i-1, j) - 2f(i, j)$, and analogously ∇_y^2 with ± 1 on j , we have that

$$\nabla_{x,y}^2 q(\pm i \pm j - a) = \begin{cases} 1 & \pm i \pm j - a \geq 0 \text{ and even;} \\ 0 & \text{otherwise;} \end{cases} \tag{22}$$

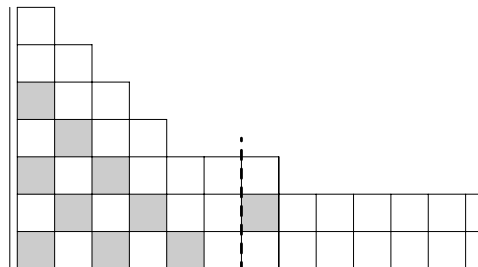
and that $\nabla_x^2 \max(0, j-a) = 1$ at $j = a$ only, while $\nabla_y^2 \max(0, j-a) = 0$ always (this reproduces the ℓ extra zeroes out of the triangles depicted in figure 5).

So, the explicit checks above can lead to the conclusion that equation (17) holds at every L for the expressions for T and Id_r given, in a special form, i.e. subtracting the equation for size L with that for size ℓ , but on the $L \times L$ system. The latter is then easily related to the one on the $\ell \times \ell$ system, at the light of equation (19a), which allows us to state that there are no different contributions from having splitted the four quadrants of $\hat{T}^{(\ell)}$. Thus, equation (19a), guessing the exact expression for T_{ij} on the edges of each quadrant by means of a simple formula, is crucial to the possibility of having the telescopic reconstruction procedure.

In other words, even without doing the tedious checks, we have seen how, by a series of manipulations corresponding to the subtraction of $\ell \times \ell$ corners to the $L \times L$ matrices, the proof is restricted to the analysis of the ‘deterministic’ part, with $i > \ell$ or $j > \ell$. As, in this case, all the involved functions depend on L through its congruence modulo 2, or 3, or 4, it suffices to check numerically the theorems for 12 consecutive sizes in order to have that the theorem must hold for all sizes. We did the explicit check for sizes up to $L = 64$.

The only thing that we need in order to conclude that the conjectured expression Id_r corresponds to the identity is to prove that it is indeed a recurrent configuration. Again, we do that in two steps, in order to divide the behaviour on the self-similar $\ell \times \ell$ corner and on the deterministic part.

First, remark that in $Id_r^{(L)}$ the internal border of the quadrant (the sites ij with i or $j = L$) is burnt in the burning test even without exploiting the other mirror images. This is true because, at every L and on both borders, we have a substructure of the form



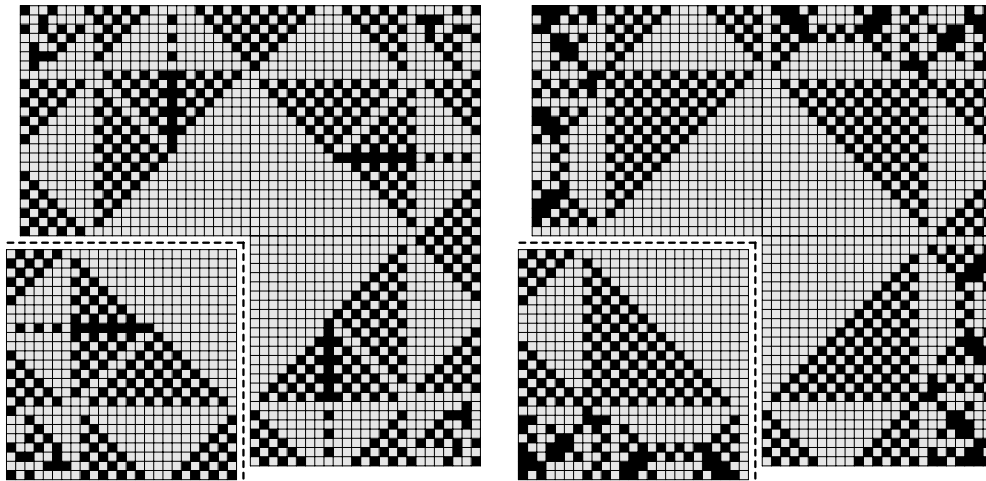
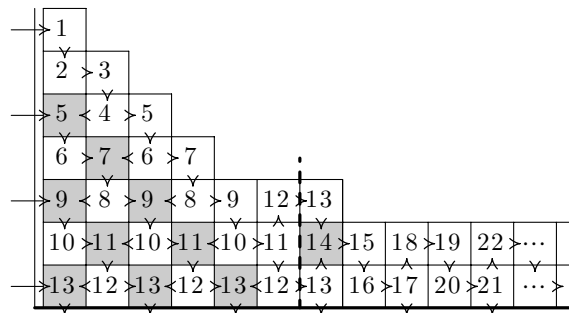


Figure 7. The recurrent identity on a portion of side 50 of the square lattice, with pseudo-Manhattan (up) and Manhattan (down) orientation.

which is burnt through the following cascade (we put the burning times, and denote with arrows from x to y a toppling occurring in x which triggers the toppling in y):



We choose to show just an example, instead of giving the explicit formula, but it should be clear from the pictures above that a general- L regular procedure exists.

So, Id_r satisfies the burning test if and only if the deterministic part of Id_r (the $L \times L$ square minus the $\ell \times \ell$ corner) satisfies the burning test with the border of the corner having a $b_{ij} = 1$ every two sites. This check must be performed only on the deterministic part, and again is done in a straightforward way, or, with conceptual economy, implied by the explicit numerical check on six consecutive sizes. This completes the proof of all the three theorems.

Manhattan lattice

For the Manhattan lattice, we performed an investigation similar to that above for the pseudo-Manhattan one, although, as we already said, the motivations are less strong, as this lattice is not planar alternating. A small-size example of the Creutz identity, compared to the pseudo-Manhattan one, is shown in figure 7.

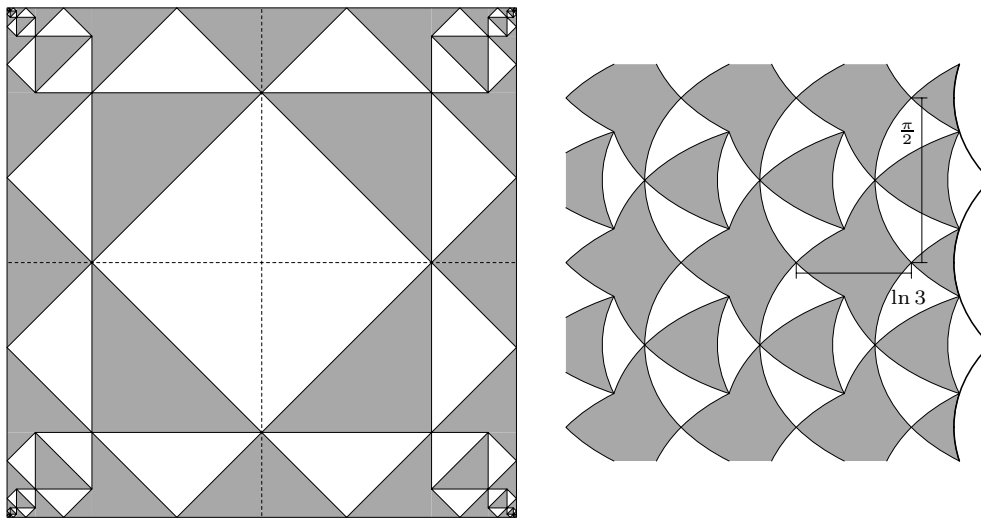


Figure 8. Up: the limit Creutz identity configuration on our Manhattan and pseudo-Manhattan lattices. White regions correspond to have height 1 almost everywhere. Grey regions correspond to have height 0 and 1 in a chequered pattern almost everywhere. Down: the image of a quadrant under the map $z \rightarrow \ln z$.

The numerics gave positive and negative results. The positive results concern the filling number k_L , that, according to extensive tests (up to $L \simeq 100$) we conjecture to be

$$k_L = \begin{cases} \frac{1}{4}L(L+2) & L \text{ even} \\ \frac{1}{4}(L+1)^2 & L \text{ odd} \end{cases} \quad (23)$$

Furthermore, the whole quadrant except for the $\ell \times (\ell - 1)$ corner seems to be deterministically described by a set of rules analogous to equations (11) (again, $\ell = \lfloor (L + 1)/3 \rfloor$), and, as in (11), depending from the congruence of L modulo 3, and a transposition involved if $s = 2$.

The negative result is that the telescopic exact self-similarity between side L and side ℓ seems to be lost in this case. As we said, this property relies crucially on the simplicity of the toppling matrix on the boundary of the quadrants, which seems to be an accidental fact of the pseudo-Manhattan lattice, and has few chances to show any universality. For this reason we did not attempt to state and prove any theorem in the fashion of theorem 1 in this case.

Conclusions

We have studied, numerically and analytically, the shape of the Creutz identity sandpile configurations, for variants of the ASM, with directed edges on a square lattice (pseudo-Manhattan and Manhattan), and square geometry. An original motivation for this study was the fact that heights are valued in $\{0, 1\}$ (while the original BTW sandpile has heights in $\{0, 1, 2, 3\}$), and we conjectured that this could led to simplifications. The results have been even simpler than expected, and qualitatively different from those in the BTW model.

In the BTW model, the exact configuration seems to be unpredictable: although some general ‘coarse-grained’ triangoloid shapes seem to have a definite large-volume limit, similar in the square geometry and in that rotated by $\pi/4$, here and there perturbations arise in the configuration, along lines and of a width of order 1 in lattice spacing. We discuss the role of these structures in various aspects of the ASM in a forthcoming paper [13].

The trianguloids have precise shapes depending from their position in the geometry, and are smaller and smaller towards the corners. Understanding analytically at least the limit shape (i.e. neglecting all the sub-extensive perturbations of the regular-pattern regions) is a task, at our knowledge, still not completed, although some first important results have been obtained in [18], and further achievements in this direction have come with the work of Levine and Peres [16, 17], both in the similar context of understanding the relaxation of a large pile in a single site (see in particular the image at page 10 of Levine thesis, and the one at

<http://math.berkeley.edu/~levine/gallery/invertedsandpile1m10x.png>,

and, for the directed model, the one at page 20 of

newton.kias.re.kr/~nspcs08/Presentation/Dhar.pdf).

In our Manhattan-like lattices on square geometry, however, we show how the situation is much simpler, and drastically different. Trianguloids are replaced by exact triangles, all of the same shape (namely, shaped as half-squares), and with straight sides. All the sides of the triangles are a fraction $\frac{1}{2}3^{-k}$ of the side of the lattice (in the limit), where the integer k is a ‘generation’ index depending on how near to a corner we are, and indeed each quadrant of the configuration is self-similar under scaling of a factor $1/3$. The corresponding ‘infinite-volume’ limit configuration is depicted in figure 8. A restatement of the self-similarity structure, in a language resembling the $z \rightarrow 1/z^2$ conformal transformation in Ostojic [18] and Levine and Peres [16], is the fact that, under the map $z \rightarrow \ln z$, a quadrant of the identity (centred at the corner) is mapped in a quasi-doubly-periodic structure.

Also the filling numbers (i.e. the minimal number of frame identities relaxing to the recurrent identity) have simple parabolic formulae, while in the original BTW model a parabola is not exact, but only a good fitting formula.

These features reach the extreme consequences in the pseudo-Manhattan lattice, where the exact configuration at some size is deterministically obtained, through a ratio- $1/3$ telescopic formula. These facts are not only shown numerically, but also proven directly in a combinatorial way.

Acknowledgments

We are grateful to an anonymous referee for many useful comments, and in particular for signalling to us a very recent paper by Dhar and collaborators [19] in which the same directed variants of the ASM as in our paper are considered, for the related problem of understanding the relaxation of a large pile of sand in a single site. This is further motivation for our work, and is quite likely to be a precious reference for future research.

References

- [1] Bak P, Tang C and Wiesenfeld K 1987 Self-organized criticality: an explanation of the $1/f$ noise *Phys. Rev. Lett.* **59** 381–4
- [2] Dhar D 1990 Self-organized critical state of sandpile automaton models *Phys. Rev. Lett.* **64** 1613–6
Dhar D 1999 The Abelian sandpile and related models *Physica A* **263** 4 (arXiv:cond-mat/9808047)
- [3] Majumdar S N and Dhar D 1991 Height correlations in the Abelian sandpile model *J. Phys. A: Math. Gen.* **24** L357–62
Majumdar S N and Dhar D 1992 Equivalence between the Abelian sandpile model and the $q \rightarrow 0$ limit of the Potts model *Physica A* **185** 129–45
- [4] Dhar D, Ruelle P, Sen S and Verma D-N 1995 Algebraic aspects of Abelian sandpile models *J. Phys. A: Math. Gen.* **28** 805–31 (arXiv:cond-mat/9408022)
- [5] Creutz M 1991 Abelian sandpiles *Comp. Phys.* **5** 198–203

- Creutz M 1991 Abelian sandpiles *Nucl. Phys. B (Proc. Suppl.)* **20** 758–61
- Bak P and Creutz M 1994 Fractals and self-organized criticality *Fractals in science* ed A Bunde and S Havlin (Berlin: Springer) pp 26–47
- [6] Sokal A D 2005 The multivariate Tutte polynomial (alias Potts model) for graphs and matroids *Surveys in Combinatorics, 2005* ed B S Webb (Cambridge: Cambridge University Press) pp 173–226 (arXiv:math/0503607)
- [7] Caracciolo S, Jacobsen J L, Saleur H, Sokal A D and Sportiello A 2004 Fermionic field theory for trees and forests *Phys. Rev. Lett.* **93** 080601 (arXiv:cond-mat/0403271)
- [8] Caracciolo S, de Grandi C and Sportiello A 2007 Renormalization flow for unrooted forests on a triangular lattice *Nucl. Phys. B* **787** 260–82 (arXiv:0705.3891)
- [9] Priezzhev V B 1993 Exact height probabilities in the Abelian sandpile model *Phys. Scr.* **T49B** 663–6
- Priezzhev V B 1994 Structure of two-dimensional sandpile. I: height probabilities *J. Stat. Phys.* **74** 955–79
- [10] Mahieu S and Ruelle P 2001 Scaling fields in the two-dimensional Abelian sandpile model *Phys. Rev. E* **64** 066130 (arXiv:hep-th/0107150)
- Ruelle P 2002 A $c = -2$ boundary changing operator for the Abelian sandpile *Phys. Lett. B* **539** 172–7 (arXiv:hep-th/0203105)
- Jeng M 2005 Conformal field theory correlations in the Abelian sandpile model *Phys. Rev. E* **71** 016140 (arXiv:cond-mat/0407115)
- Moghim-Araghi S, Rajabpour M A and Rouhani S 2005 Abelian sandpile model: a conformal field theory point of view *Nucl. Phys. B* **718** 362–70 (arXiv:cond-mat/0410434)
- Piroux G and Ruelle P 2004 Pre-logarithmic and logarithmic fields in a sandpile model *J. Stat. Mech.* P10005 (arXiv:hep-th/0407143)
- Piroux G and Ruelle P 2005 Boundary height fields in the Abelian sandpile model *J. Phys. A: Math. Gen.* **38** 1451–72 (arXiv:hep-th/0409126)
- Piroux G and Ruelle P 2005 Logarithmic scaling for height variables in the Abelian sandpile model *Phys. Lett. B* **607** 188–96 (arXiv:cond-mat/0410253)
- [11] Jeng M, Piroux G and Ruelle P 2006 Height variables in the Abelian sandpile model: scaling fields and correlations *J. Stat. Mech.* P10015 (arXiv:cond-mat/0609284)
- Poghosyan V S, Grigorev S Y, Priezzhev V B and Ruelle P 2008 Pair correlations in sandpile model: a check of logarithmic conformal field theory *Phys. Lett. B* **659** 768–72 (arXiv:0710.3051)
- [12] Creutz M 1996 Xtoys: cellular automata on xwindows *Nucl. Phys. B (Proc. Suppl.)* **47** 846–9 (arXiv:hep-lat/9508029) (code: <http://thy.phy.bnl.gov/www/xtoys/xtoys.html>)
- [13] Caracciolo S, Paoletti G and Sportiello A Pseudo-propagators and other geometric structures in the Abelian sandpile (at press)
- [14] Caracciolo S, Causo M S, Grassberger P and Pelissetto A 1999 Determination of the exponent γ for SAWs on the two-dimensional Manhattan lattice *J. Phys. A: Math. Gen.* **32** 2931–48 (arXiv:cond-mat/9812267)
- [15] Chalker J T and Coddington P D 1988 Percolation, quantum tunnelling and the integer Hall effect *J. Phys. C: Solid State Phys.* **21** 2665–79
- [16] Levine L and Peres Y 2007 Scaling limits for internal aggregation models with multiple sources (arXiv:0712.3378)
- [17] Levine L 2007 *PhD Dissertation Thesis* University California at Berkeley, fall (arXiv:0712.4358) (<http://math.berkeley.edu/~levine/levine-thesis.pdf>)
- [18] Ostojic S 2003 Patterns formed by addition of grains to only one site of an Abelian sandpile *Physica A* **318** 187–99
- [19] Dhar D, Sadhu T and Chandra S 2008 Pattern formation in growing sandpiles *Phys. Rev. Lett.* (arXiv:0808.1732) (at press)